

## Article

# Electrical Stimuli-Responsive Decomposition of Layer-by-Layer Films Composed of Polycations and TEMPO-Modified Poly(acrylic acid)

Kentaro Yoshida <sup>1,\*</sup>, Toshio Kamijo <sup>2</sup>, Tetsuya Ono <sup>1</sup>, Takenori Dairaku <sup>3</sup>, Shigehiro Takahashi <sup>4</sup>, Yoshitomo Kashiwagi <sup>1</sup> and Katsuhiko Sato <sup>5</sup>

- <sup>1</sup> School of Pharmaceutical Sciences, Ohu University, 31-1 Misumido, Tomita-machi, Koriyama 963-8611, Fukushima, Japan
- <sup>2</sup> Department of Creative Engineering, National Institute of Technology, Tsuruoka College, 104 Sawada, Inooka, Tsuruoka 997-8511, Yamagata, Japan
- <sup>3</sup> Integrated Center for Science and Humanities, The Section of Chemistry, Fukushima Medical University, 1 Hikarigaoka, Fukushima City 960-1295, Fukushima, Japan
- <sup>4</sup> Faculty of Pharmacy, Takasaki University of Health and Welfare, 37-1 Nakaorui-cho, Takasaki 370-0033, Gunma, Japan
- <sup>5</sup> Faculty of Pharmaceutical Science, Tohoku Medical and Pharmaceutical University, 4-4-1 Komatsushima, Aoba, Sendai 981-8558, Miyagi, Japan
- \* Correspondence: k-yoshida@pha.ohu-u.ac.jp; Tel.: +81-24-932-8931

**Abstract:** We previously reported that layer-by-layer (LbL) film prepared by a combination of 2,2,6,6-tetramethylpiperidiny1 *N*-oxyl (TEMPO)-modified polyacrylic acid (PAA) and polyethyleneimine (PEI) were decomposed by application of an electric potential. However, there have been no reports yet for other polycationic species. In this study, LbL films were prepared by combining various polycationics (PEI, poly(allylamine hydrochloride) (PAH), poly(diallyldimethylammonium chloride) (PDDA), and polyamidoamine (PAMAM) dendrimer) and TEMPO-PAA, and the decomposition of the thin films was evaluated using cyclic voltammetry (CV) and constant potential using an electrochemical quartz crystal microbalance (eQCM). When a potential was applied to an electrode coated on an LbL thin film of polycations and TEMPO-PAA, an oxidation potential peak ( $E_p^a$ ) was obtained around +0.6 V vs. Ag/AgCl in CV measurements. EQCM measurements showed the decomposition of the LbL films at voltages near the  $E_p^a$  of the TEMPO residues. Decomposition rate was 82% for the (PEI/TEMPO-PAA) film, 52% for the (PAH/TEMPO-PAA)<sub>5</sub> film, and 49% for the (PDDA/TEMPO-PAA)<sub>5</sub> film. It is considered that the oxoammonium ion has a positive charge, and the LbL films were decomposed due to electrostatic repulsion with the polycations (PEI, PAH, and PDDA). These LbL films may lead to applications in drug release by electrical stimulation. On the other hand, the CV of the (PAMAM/TEMPO-PAA)<sub>5</sub> film did not decompose. It is possible that the decomposition of the thin film is not promoted, probably because the amount of TEMPO-PAA absorbed is small.

**Keywords:** layer-by-layer; multilayer film; thin layer film; electro-decomposition; DDS; TEMPO



**Citation:** Yoshida, K.; Kamijo, T.; Ono, T.; Dairaku, T.; Takahashi, S.; Kashiwagi, Y.; Sato, K. Electrical Stimuli-Responsive Decomposition of Layer-by-Layer Films Composed of Polycations and TEMPO-Modified Poly(acrylic acid). *Polymers* **2022**, *14*, 5349. <https://doi.org/10.3390/polym14245349>

Academic Editor: Zhengzhong Zhou

Received: 10 November 2022

Accepted: 5 December 2022

Published: 7 December 2022

**Publisher's Note:** MDPI stays neutral with regard to jurisdictional claims in published maps and institutional affiliations.



**Copyright:** © 2022 by the authors. Licensee MDPI, Basel, Switzerland. This article is an open access article distributed under the terms and conditions of the Creative Commons Attribution (CC BY) license (<https://creativecommons.org/licenses/by/4.0/>).

## 1. Introduction

Stimuli-sensitive systems such as gels, thin films, and microcapsules have been studied for their various applications in fields including biomaterials, energy storage and conversion. To achieve such a functional application, techniques to combine predictable responses to stimuli-materials, and controlled composition and nanostructural have been reported [1,2]. A diversity of polyelectrolytes has been used in the research on many nanostructured systems. As stimulus-responsive polymers, synthetic polymers modified with functional substances and enzymes of biomaterials have been reported in fields such

as biology, organics, and polymer chemistry [3–5]. In addition, layer-by-layer (LbL) deposition is attracting attention as a combination of functional polymers and nanostructures. Functional polymers for LbL films include synthetic polymers, polysaccharides, proteins, and DNA [6–8]. Thin films can have various functions through the use of such functional polymers. In particular, LbL films have been used as stimuli-responsive thin films for stimuli such as pH [9], ionic strength [10], electrochemical stimulus [11,12], temperature [13], sugars [14,15], and hydrogen peroxide [16]. In the case of pH and ionic strength stimuli-responsive thin films, the charge density of the weak polyelectrolyte functional species changes with the pH and ionic strength of the solvent. In particular, thin films composed of amphoteric polyelectrolytes with weak positive and negative charges can be decomposed by a pH-trigger [17]. We have recently prepared LbL films by combining glucose oxidase, DNA, and hemin, and reported thin film decomposition in response to sugar and hydrogen peroxide [18–20].

In the case of electrical stimuli-responsive thin films, there are reports of the use of redox polymers and indefinite nanoparticles. For example, ferrocene-modified polymers can be decomposed by the application of an oxidizing potential in thin films based on the redox-active components of LbL films [21]. In addition, redox active substances such as alizarin red, polypyrrole, and metal nanoparticles are also used in LbL films with redox activity [22–24]. Electrostimuli-responsive films are expected to be applied to biosensors and drug delivery systems (DDS), such as with the electrochemical decomposition/swelling of thin films.

Our study is focused on 2,2,6,6-tetramethylpiperidiny1 *N*-oxyl (TEMPO) derivatives. The TEMPO derivative is a stable nitroxide radical that is often used as a catalyst for various oxidative transformations (alcohol oxidation, oxygen reduction, and various organic reactions [25–27]). One-electron oxidation of nitroxides produces oxoammonium cations that provide active oxidants (Figure 1) [28].

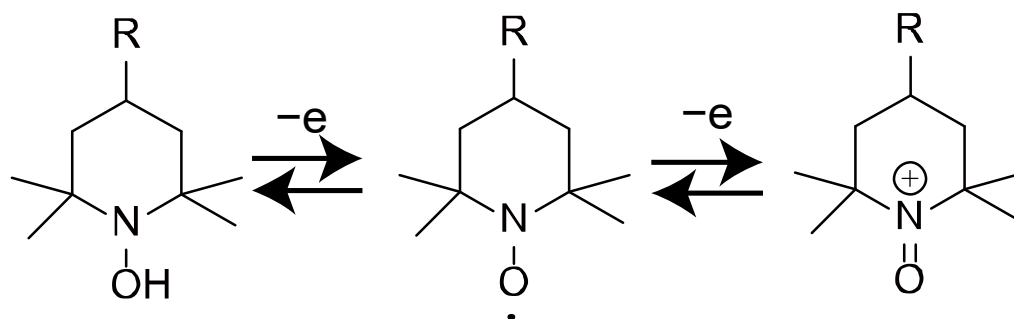


**Figure 1.** Reversible redox system based on nitroxyl radicals.

The oxoammonium cation can be used in stoichiometric quantities or generated electrochemically in situ, or through the use of a variety of secondary oxidants [29]. Therefore, in the case of LbL films driven by electrostatic interactions, the stability of thin films composed of TEMPO derivatives should be dependent on the electrode potential. We previously reported that LbL films prepared by a combination of TEMPO-modified polyacrylic acid (PAA) and polyethyleneimine (PEI) were decomposed by application of an electric potential [30]. This is due to the oxidation of the TEMPO derivative, and the increase in the positive charge density of the weak polyelectrolyte degrades the balance of the thin film driven by the electrostatic interaction, which leads to decomposition of the LbL film (Figure 2).

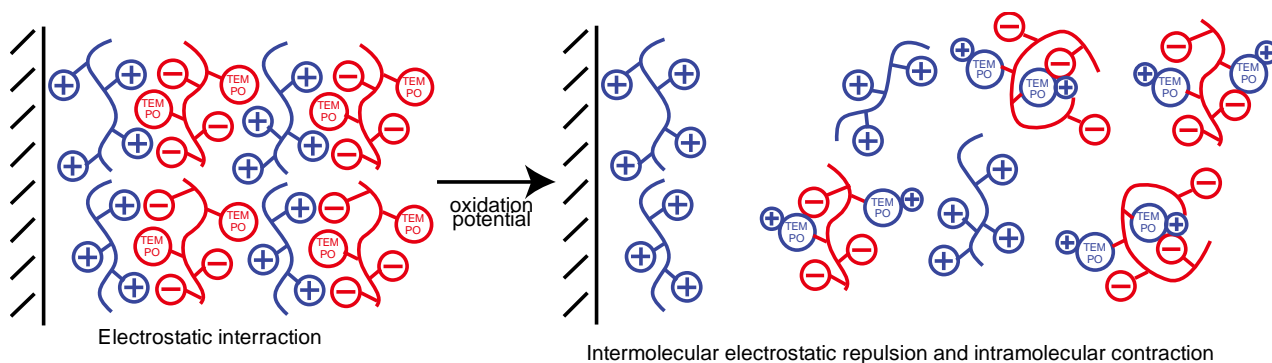


**Figure 2.** Response of TEMPO-PAA and polycations to electrical-stimulation. Schematic depiction of the molecular and conformational responses of polyelectrolytes bearing either basic, acid, or TEMPO moieties with respect to electrical-stimuli.

However, there have been no reports yet for other polycationic species. Elucidating the positive charge state of primary and quaternary amines and the degradability of thin films in linear and branched polymers may lead to applications in drug release upon electrical stimulation. In this study, LbL membranes were prepared by combining various polycationics (PEI, poly(allylamine hydrochloride) (PAH), poly(diallyldimethylammonium chloride) (PDDA), and polyamidoamine (PAMAM) dendrimer) and TEMPO-PAA, and the decomposition of the thin films was evaluated using cyclic voltammetry (CV) and constant potential using an electrochemical quartz crystal microbalance (eQCM). Furthermore, the fluorescence intensity of solutions in which the thin films were degraded was measured using fluorescein isothiocyanate (FITC)-labeled polycations as a drug model compound.

## 2. Materials and Methods

### 2.1. Materials

Poly(acryloyl chloride) (25% soln. in dioxane) was purchased from Polysciences Inc. (Warrington, PA, USA). 4-Amino-2,2,6,6-tetramethylpiperidine *N*-oxyl free radical (4-amino-TEMPO) was purchased from Tokyo Chemical Inc. (Tokyo, Japan). PAH (average MW: 150,000) and PEI (MW: 60,000–80,000) were obtained from Nittbo Co. (Tokyo, Japan) and Nacalai Tesque Inc. (Tokyo, Japan)). PDDA (MW: 100,000–200,000), PAMAM dendrimer (ethylenediamine core, generation 4.0), and FITC isomer I were obtained from Sigma-Aldrich, Co (Saint Louis, MO, USA).

TEMPO-PAA was synthesized as follows. Poly(acryloyl chloride) (100 mg), 4-amino-TEMPO (80 mg), and triethylamine (80  $\mu$ L) were mixed in 5 mL of dioxane for 24 h. Ten milliliters of water was added to the reaction mixture to and stirred for 24 h. The product was purified by dialysis with milliQ water for 3 days. The TEMPO-PAA contained approximately 35% 4-amino TEMPO residues as calculated from the proportions of nitrogen and carbon determined by elemental analysis (C, 55.67%; H, 8.31%; N, 7.43%). The chemical structures of TEMPO-PAA, PEI, PAH, PAMAM, and PDDA are shown in Figure 3. FITC-labeled polycations (FITC-PEI, FITC-PAH, and FITC-PAMAM) were synthesized as follows. The various polycations (100 mg) and FITC (amount that modifies 1% of primary amines contained in various polyanions) were mixed in an aqueous solution at 4  $^{\circ}$ C for over 12 h. The product was purified by dialysis with milliQ water for 3 days.

### 2.2. Analyses

A quartz crystal microbalance (QCM; QCA 917 system, Seiko EG&G, Tokyo, Japan) was employed for gravimetric analysis of the dried LbL films consisting of polycations and TEMPO-PAA. A 9 MHz AT-cut quartz resonator coated with a gold (Au) layer (surface area 0.4 cm<sup>2</sup>) was used as a probe. An eQCM (eQCM 10M, Gamry, Warminster, UK) was used for gravimetric analysis of the wet LbL films. An 8 MHz AT-cut quartz resonator coated with a thin Au layer (0.2 cm<sup>2</sup>) was used as a probe. Atomic force microscopy (AFM;

AFM5200S, Hitachi High-Technologies Co., Tokyo, Japan) images were acquired in contact mode at room temperature and in air. An electrochemical analyzer (ALS model 1200B, BAS Inc., Tokyo, Japan) was used for cyclic voltammetry and application of a constant potential. Fluorescence spectroscopy measurements were conducted using a fluorescence spectrophotometer (RF-1500, Shimadzu Co., Kyoto, Japan). UV-vis spectroscopy measurements were conducted using a UV-3100PC (Shimadzu Co., Kyoto, Japan) spectrometer.

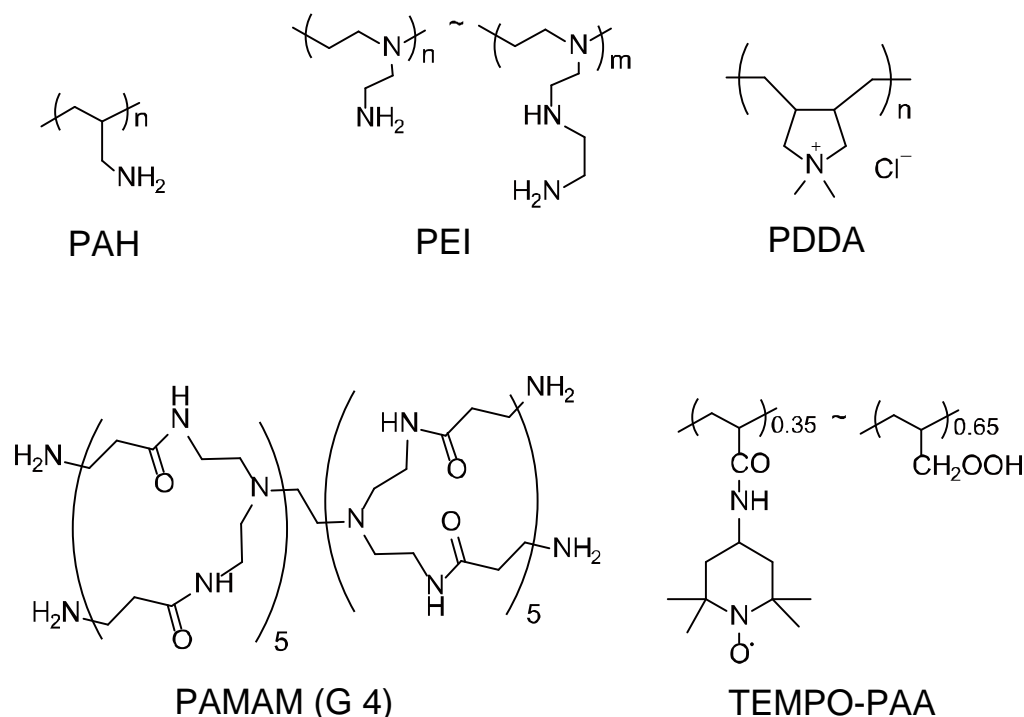


**Figure 3.** Chemical structures of PAH, PEI, PDDA, PAMAM and TEMPO-PAA.

### 2.3. Preparation of LbL Films

LbL films were prepared on a solid substrate (Au-coated quartz resonator for eQCM analysis), quartz slide (50 × 9 × 1 mm) and glassy carbon electrode (GCE) slides for constant potential application. The solid substrates were alternately immersed in 0.1 mg/mL polycation solution and 0.1 mg/mL TEMPO-PAA solution for 15 min. The slides were rinsed with a working buffer for 5 min to remove any weakly adsorbed polycations and TEMPO-PAA. The deposition was repeated to build up LbL films. All experiments were conducted at room temperature.

Deposition was repeated to construct the LbL films on a 9-MHz Au-coated quartz resonator (surface area 0.4 cm<sup>2</sup>), after which the films were rinsed with water, and the change in the resonance frequency of the dry film was recorded after each deposition to determine its weight. In addition, the surface morphology of the dry film was recorded using AFM in contact mode.

### 2.4. Cyclic Voltammetry and Constant Potential Application

Cyclic voltammograms (CVs) and eQCM (8-MHz Au-coated quartz resonator, surface area 0.2 cm<sup>2</sup>) were recorded in a conventional three-electrode system using a stainless steel tube counter electrode and Ag/AgCl reference electrode (eQCM flow cell kit, BAS Inc., Tokyo, Japan). All measurements were performed. The LbL film-coated Au quartz resonator was immersed in 10 mM HEPES buffer (pH 7.0, 150 mM NaCl) for 10 min. The electrode potential of the Au-coated resonator was scanned from +0 to +0.8 V at 0.05 V/s, and constant potentials of 0, +0.4, +0.6, and +0.8 V were applied for 10 min. The eQCM was measured while the potential was applied to the quartz resonator.

### 2.5. Release of FITC-Polycation Due to Constant Potential Application Obtained from the (FITC-Polycation/TEMPO-PAA)<sub>5</sub> Films-Coated Electrodes

To release FITC-polycations (FITC-PEI, FITC-PAH, and FITC-PAMAM), electrode potentials from +0 to +0.8 V were applied to the (FITC-polycation/TEMPO-PAA)<sub>5</sub> film-coated GCEs (50 × 9 × 1 mm) in 10 mM HEPES buffer (pH 7.0, 150 mM NaCl). The constant potential of the film-coated GCEs was applied in a conventional three-electrode system using a platinum wire counter electrode and an Ag/AgCl reference electrode.

The fluorescence intensity of the FITC-polycations released from the LbL films was determined at 520 nm using a fluorescence spectrophotometer with an excitation wavelength of 490 nm. Release of the FITC-polycations was calculated based on the fluorescence intensity of the solution in which a potential was applied to the LbL film-coated GCEs for a predetermined time. A calibration graph obtained using the fluorescence intensity of free FITC-polycations was used.

## 3. Results

### 3.1. Preparation of (Polycation/TEMPO-PAA)<sub>n</sub> Films

We have previously reported that multilayer films can be formed by LbL deposition utilizing the electrostatic interaction between polymers [31]. Here, we evaluate whether or not polycations and TEMPO-PAA also form multilayer films. Figure 4 shows the change in the resonance frequency ( $\Delta F$ ) of QCM measurements observed during the deposition of polycations and TEMPO-PAA on a Au-coated 9 MHz quartz resonator (surface area: 0.4 cm<sup>2</sup>). When the thin film is dried, the frequency change of the probe can be obtained from the Sauerbrey equation to determine the mass deposited onto the quartz resonator; the deposition of 1 ng of a substance induces a  $-0.91$  Hz change in the resonance frequency. The amount of deposited LbL film was calculated to be ca.  $3.41 \pm 0.54$   $\mu\text{g}/\text{cm}^2$  for the (PAH/TEMPO-PAA)<sub>5</sub> film, ca.  $3.16 \pm 0.21$   $\mu\text{g}/\text{cm}^2$  for the (PEI/TEMPO-PAA)<sub>5</sub> film, ca.  $2.13 \pm 0.29$   $\mu\text{g}/\text{cm}^2$  for the (PAMAM/TEMPO-PAA)<sub>5</sub> film, and ca.  $2.02 \pm 0.16$   $\mu\text{g}/\text{cm}^2$  for the (PDDA/TEMPO-PAA)<sub>5</sub> film. The difference in the film formation of each polycation will be described later; however, the formation of LbL films with TEMPO-PAA was possible for all polycations.

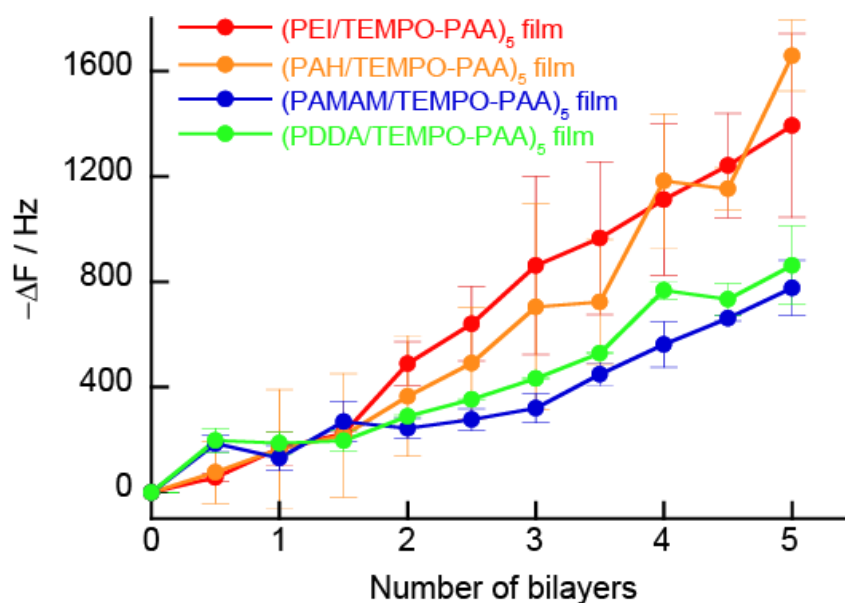


**Figure 4.** QCM resonator frequency changes during drying of the prepared (PEI/TEMPO-PAA)<sub>n</sub> (red), (PAH/TEMPO-PAA)<sub>n</sub> (orange), (PAMAM/TEMPO-PAA)<sub>n</sub> (blue), and (PDDA/TEMPO-PAA)<sub>n</sub> (green) films. Surface area: 0.4 cm<sup>2</sup>.

To further verify the LbL film preparation, AFM observations of dried (PEI/TEMPO-PAA)<sub>5</sub>, (PAH/TEMPO-PAA)<sub>5</sub>, (PAMAM/TEMPO-PAA)<sub>5</sub>, and (PDDA/TEMPO-PAA)<sub>5</sub> films were conducted (Figure 5). The roughness values ranged from 68.0 nm for the (PEI/TEMPO-PAA)<sub>5</sub> film, 65.7 nm for the (PAH/TEMPO-PAA)<sub>5</sub> film, 61.7 nm for the (PAMAM/TEMPO-PAA)<sub>5</sub> film, and 9.19 nm for the (PDDA/TEMPO-PAA)<sub>5</sub> film. All the obtained LbL films have TEMPO-PAA as the outermost layer, and the surface morphology was similar. Many examples of LbL films surface roughness on the scale of several tens of nm have been reported [18,30]. These results are presumed to be similar to the adsorption of polymers in the LbL films.

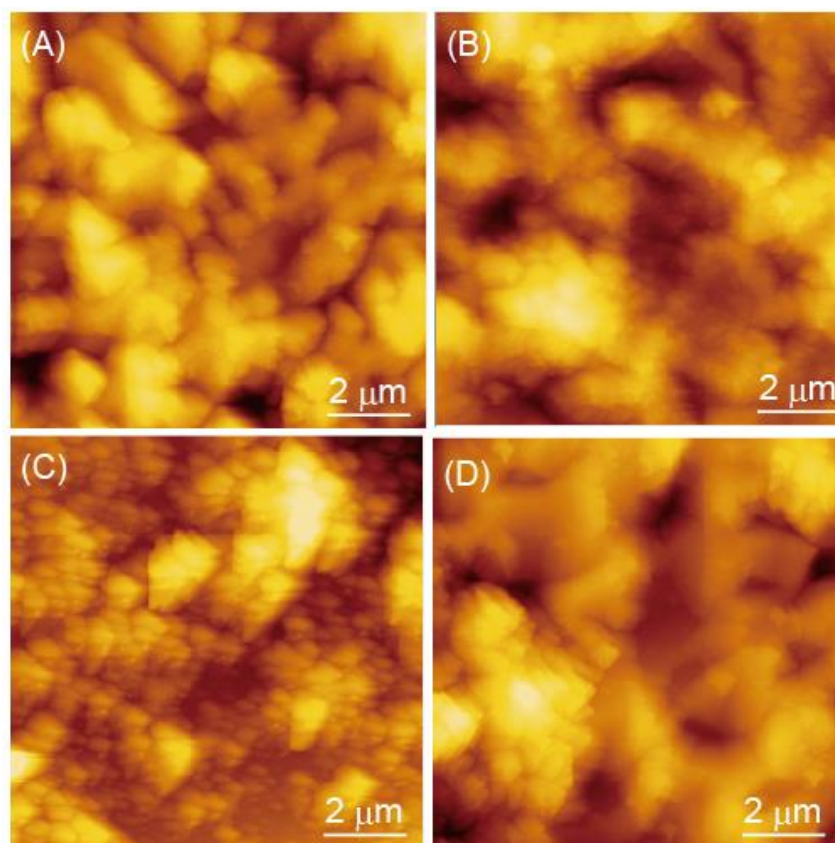


**Figure 5.** AFM images of dried (A) (PEI/TEMPO-PAA)<sub>5</sub>, (B) (PAH/TEMPO-PAA)<sub>5</sub>, (C) (PAMAM/TEMPO-PAA)<sub>5</sub>, and (D) (PDDA/TEMPO-PAA)<sub>5</sub> films.

### 3.2. Electrical Stimuli-Responsive Decomposition of (Polycation/TEMPO-PAA)<sub>5</sub> Film-Coated Electrodes

The dried (PEI/TEMPO-PAA)<sub>5</sub> film was immersed in the buffer solution and a potential was applied using CV. However, the frequency change in the dry QCM measurement and the surface state in the AFM observation did not change. For dried LbL films, the AFM thickness values are known to be much lower than those obtained for wet LbL films [32,33]. This may be due to the increase in the density of the thin film, which also made it difficult to decompose the thin film. Therefore, in all subsequent experiments, the decomposition of the thin film, which is possible in solution, was investigated by application of an electric potential using a flow-type QCM.

#### 3.2.1. CVs and eQCM Measurements Obtained from (PEI/TEMPO-PAA)<sub>5</sub> Film-Coated Electrodes

Figure 6 shows CVs and eQCM measurements obtained for the (PEI/TEMPO-PAA)<sub>5</sub> film-modified quartz resonator. The CVs contain an oxidation peak at +0.6 V due to the oxidation reaction of TEMPO in the (PEI/TEMPO-PAA)<sub>5</sub> film. An oxidation current peak

( $I_p^a$ ) of 74  $\mu\text{A}$  was observed at an oxidation potential peak ( $E_p^a$ ) of +0.64 V in the 1st sweep. However, a significant decrease in  $I_p^a$  was observed after the 2nd sweep. The corresponding eQCM measurement showed a sharp increase in  $\Delta F$  around +0.6 V during the 1st sweep.  $\Delta F$  after the sweep scan showed an increase of approximately +690 Hz. The increased  $\Delta F$  shows that approximately 82% of the weight of the (PEI/TEMPO-PAA)<sub>5</sub> film was removed from the Au-coated quartz resonator because the adsorption of the LbL film caused a change in  $\Delta F$  of  $-842$  Hz. From the eQCM changes after the 2nd sweep, it can be inferred that all the TEMPO-PAA that could be resolved in the 1st sweep was exfoliated from the quartz resonator (Note: the layer of polyelectrolyte directly adsorbed on the substrate is not exfoliated).

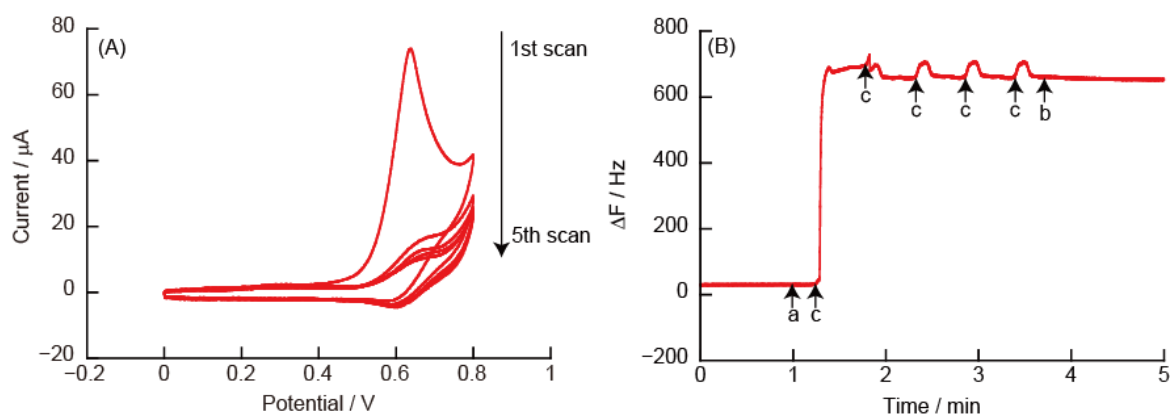


**Figure 6.** (A) Cyclic voltammograms of (PEI/TEMPO-PAA)<sub>5</sub> film in 10 mM HEPES (pH 7, containing 150 mM NaCl), and (B) changes in the resonance frequency on the Au resonator in eQCM. The electric potential (scan rate: 50 mV/s, number of sweep scan: 5 cycles) was applied between (a) and (b) in the eQCM, and (c) indicates an oxidation potential of +0.6 V.

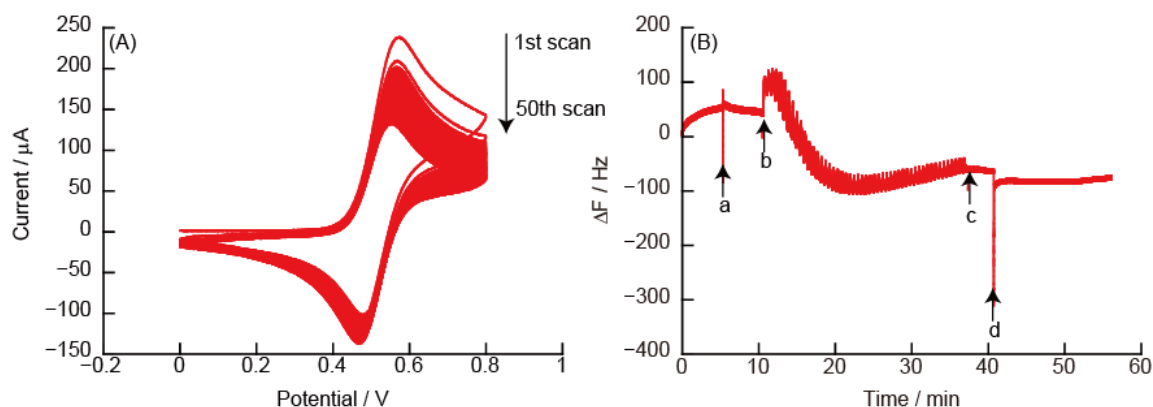
The mechanism of LbL film decomposition is as follows. The TEMPO residues were electrochemically oxidized at +0.6 to +0.7 V to form positively charged oxoammonium ions. We have reported that the decomposition of the film is probably caused by electrostatic repulsion between the positively charged oxoammonium ions and PEI [30]. Sodium hypochlorite is used to oxidize TEMPO. The absorbance spectra of the LbL films decreased significantly when the (PEI/TEMPO-PAA) films were immersed in sodium hypochlorite solution (Figure S1). It is assumed that the LbL film decomposed due to the oxidation of the TEMPO derivative.

The usefulness of the LbL film composed of polycations with covalently modified TEMPO is discussed here. Figure 7 shows CVs and eQCM measurements obtained from the (PEI/PAA)<sub>5</sub> film-modified Au electrode in 10 mM TEMPO solution. The CVs indicated a reversible redox response of TEMPO for 50 sweep scans. However, no increase in  $\Delta F$  was observed in the eQCM measurements, i.e., the LbL film does not decompose. PAA with covalently modified TEMPO increases the intramolecular positive charge depending on the oxidation potential. The change in the charge of the polymer in the thin film disturbs the balance of the electrostatic interaction, which is the driving force that constitutes the LbL films, and this causes the LbL film to decompose.

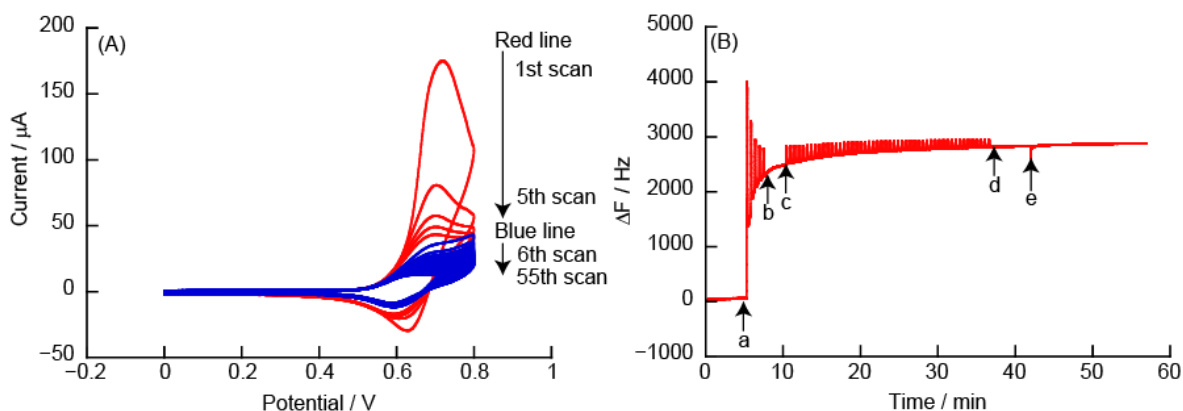
### 3.2.2. CVs and eQCM Measurements Obtained from (PAH/TEMPO-PAA)<sub>5</sub> Film-Coated Electrodes

Figure 8 shows CVs and eQCM measurements obtained for the (PAH/TEMPO-PAA)<sub>5</sub> film-modified Au electrode. The CVs show  $E_p^a$  at +0.7 V due to the oxidation reaction of TEMPO in the (PAH/TEMPO-PAA)<sub>5</sub> film. At  $E_p^a$  in the 1st scan,  $\Delta F$  in the eQCM measurement increased due to the oxidation reaction of the (PEI/TEMPO-PAA)<sub>5</sub> film. Similar to the (PAH/TEMPO-PAA)<sub>5</sub> film, the increase in  $\Delta F$  involves the decomposition of the (PAH/TEMPO-PAA)<sub>5</sub> film. The  $I_p^a$  in the CV after the 2nd scan decreased significantly

compared to that of the 1st scan, and the rate of change with the increase in  $\Delta F$  decreased. After the 5th scan,  $\Delta F$  showed an increase of approximately +2450 Hz. After an additional 50 scans,  $\Delta F$  showed a total increase of ca. +2880 Hz. The adsorption of the (PAH/TEMPO-PAA)<sub>5</sub> film caused a change in  $\Delta F$  of −5630 Hz, i.e., approximately 52% of weight of the (PAH/TEMPO-PAA)<sub>5</sub> film was removed from the Au-coated quartz resonator. The (PAH/TEMPO-PAA)<sub>5</sub> film thus decomposes similarly to the (PEI/TEMPO-PAA)<sub>5</sub> film.



**Figure 7.** (A) Cyclic voltammograms of (PEI/PAA)<sub>5</sub> film in 10 mM TEMPO solution, and (B) changes in the resonance frequency on the Au resonator in the eQCM. During QCM measurements, the Au resonator was exposed in (a) 10 mM TEMPO solution and (d) working buffer. The electric potential (scan rate: 50 mV/s, number of sweep scan: 5 cycles) was applied between (b) and (c) in the eQCM.



**Figure 8.** (A) Cyclic voltammograms of (PAH/TEMPO-PAA)<sub>5</sub> film in 10 mM HEPES (pH 7, containing 150 mM NaCl), and (B) changes in the resonance frequency on the Au resonator in the eQCM. The electric potential (scan rate: 50 mV/s) was applied between (a) and (b) (number of sweep scan: 5 times), or (c) and (d) (number of sweep scan: 50 times) in the eQCM. Finally, the Au resonator was exposed to 10 mM HEPES buffer (pH 7, containing 150 mM NaCl) (e).

### 3.2.3. CVs and eQCM Measurements Obtained from (PDDA/TEMPO-PAA)<sub>5</sub> Film-Coated Electrodes

PDDA is a high charge density cationic polymer with quaternary amines. Figure 9 shows CVs and eQCM measurements obtained from the (PDDA/TEMPO-PAA)<sub>5</sub> film-coated Au electrode. The CVs show  $E_{p^a}$  at +0.6 V due to the oxidation reaction of TEMPO in the (PDDA/TEMPO-PAA)<sub>5</sub> film. At  $E_{p^a}$  in the 1st scan,  $\Delta F$  from the eQCM measurements increased due to the oxidation reaction of the (PDDA/TEMPO-PAA)<sub>5</sub> film. In the 2nd and subsequent scans,  $I_{p^a}$  was significantly decreased and there was no change in  $\Delta F$  compared to that of the 1st scan. This shows a tendency similar to that of the (PEI/TEMPO-PAA)<sub>5</sub> film. After the 55th scan,  $\Delta F$  showed an increase of approximately +208 Hz. Figure 9B shows that approximately 49% of the mass of the (PDDA/TEMPO-PAA)<sub>5</sub> film was removed from

the Au-coated quartz resonator because the adsorption of the (PDDA/TEMPO-PAA)<sub>5</sub> film caused a change in  $\Delta F$  of  $-421$  Hz.

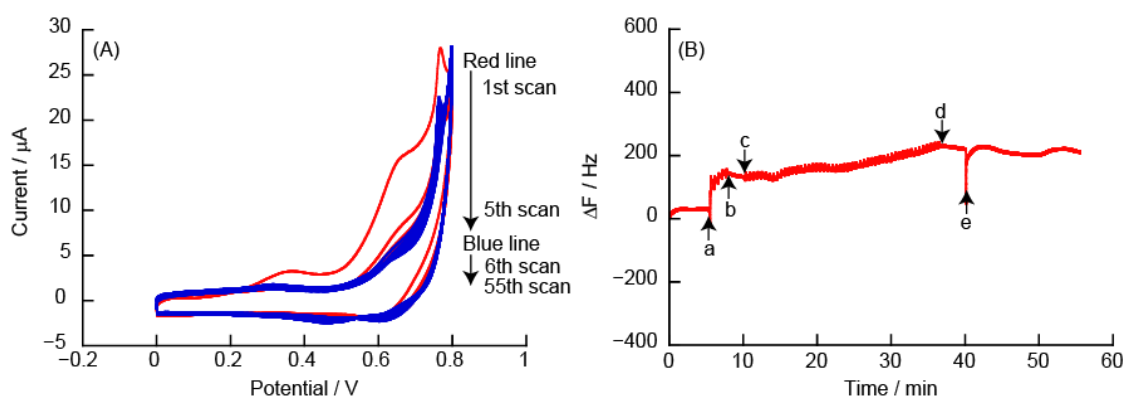


**Figure 9.** (A) Cyclic voltammograms of (PDDA/TEMPO-PAA)<sub>5</sub> film in 10 mM HEPES (pH 7, containing 150 mM NaCl), and (B) changes in the resonance frequency on the Au resonator in eQCM. The electric potential (scan rate: 50 mV/s) was applied between (a) and (b) (number of sweep scan: 5 times), or (c) and (d) (number of sweep scan: 50 times) in the eQCM. Finally, the Au resonator was exposed to 10 mM HEPES buffer (pH 7, containing 150 mM NaCl) (e).

### 3.2.4. CVs and eQCM Measurements Obtained from (PAMAM/TEMPO-PAA)<sub>5</sub> Film-Coated Electrodes

PAMAM is a spherical macromolecule that can sequester low molecular weight compounds in cavities, and PAMAM has been extensively studied as a drug carrier for DDS [34,35]. If the membrane that includes PAMAM can be decomposed electrochemically, it may be applicable to DDS. Figure 10 shows CVs and eQCM measurements obtained from the (PAMAM/TEMPO-PAA)<sub>5</sub> film-modified Au electrode. The CVs show  $Ep^a$  at  $+0.6$  V due to the oxidation reaction of TEMPO in the (PAMAM/TEMPO-PAA)<sub>5</sub> film during the 1st scan. The adsorption of the (PAMAM/TEMPO-PAA)<sub>5</sub> film caused a change in  $\Delta F$  of  $-710$  Hz, which was approximately the same amount of change in  $\Delta F$  as the (PEI/TEMPO-PAA)<sub>5</sub> film. However,  $Ip^a$  in the 1st sweep scan of the (PAMAM/TEMPO-PAA)<sub>5</sub> film was ca.  $7$   $\mu A$ , which is significantly smaller than that of the (PEI/TEMPO-PAA)<sub>5</sub> film. Therefore, even if the amount of change in  $\Delta F$  is the same, the amount of adsorption of TEMPO-PAA is small. Alternatively, the film may be in a state where it cannot be oxidized and reduced.

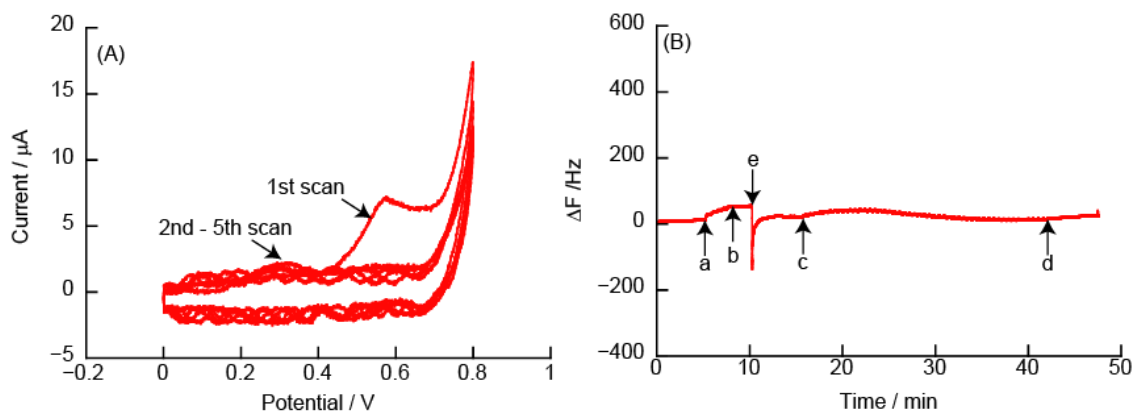


**Figure 10.** (A) Cyclic voltammograms of (PAMAM/TEMPO-PAA)<sub>5</sub> film in 10 mM HEPES (pH 7, containing 150 mM NaCl), and (B) changes in the resonance frequency on the Au resonator. The electric potential (scan rate: 50 mV/s) was applied between (a) and (b) (number of sweep scan: 5 times), or (c) and (d) (number of sweep scan: 50 times) in the eQCM. The Au resonator was exposed to 10 mM HEPES buffer (pH 7, containing 150 mM NaCl) (e).

### 3.2.5. Changes in Resonance Frequency Due to Application of a Constant Potential

The decomposition of LbL films at constant potential was investigated. Figure 11 shows the changes in the resonance frequency upon application of +0.4, +0.6, and +0.8 V to the (PEI/TEMPO-PAA)<sub>5</sub>, (PAH/TEMPO-PAA)<sub>5</sub>, (PDDA/TEMPO-PAA)<sub>5</sub>, and (PAMAM/TEMPO-PAA)<sub>5</sub> film-coated electrodes. In the electrode coated with the (PEI/TEMPO-PAA)<sub>5</sub> and (PAH/TEMPO-PAA)<sub>5</sub> films, the change in  $\Delta F$  was slight when a potential of +0.4 V was applied, but an increase in  $\Delta F$  was observed when a potential greater than +0.6 V was applied. The decomposition rate was calculated from the amount of change in  $\Delta F$ , which indicated the decomposition of the (PEI/TEMPO-PAA)<sub>5</sub> and (PAH/TEMPO-PAA)<sub>5</sub> films was ca. 50% and 30% at +0.6 V, and ca. 90% and 79% at +0.8 V, respectively. Decomposition of the (PDDA/TEMPO-PAA)<sub>5</sub> film was also observed at +0.8 V. On the other hand, the PAMAM film that was not decomposed during the CV measurements was not decomposed even by application of a constant potential of +0.8 V.

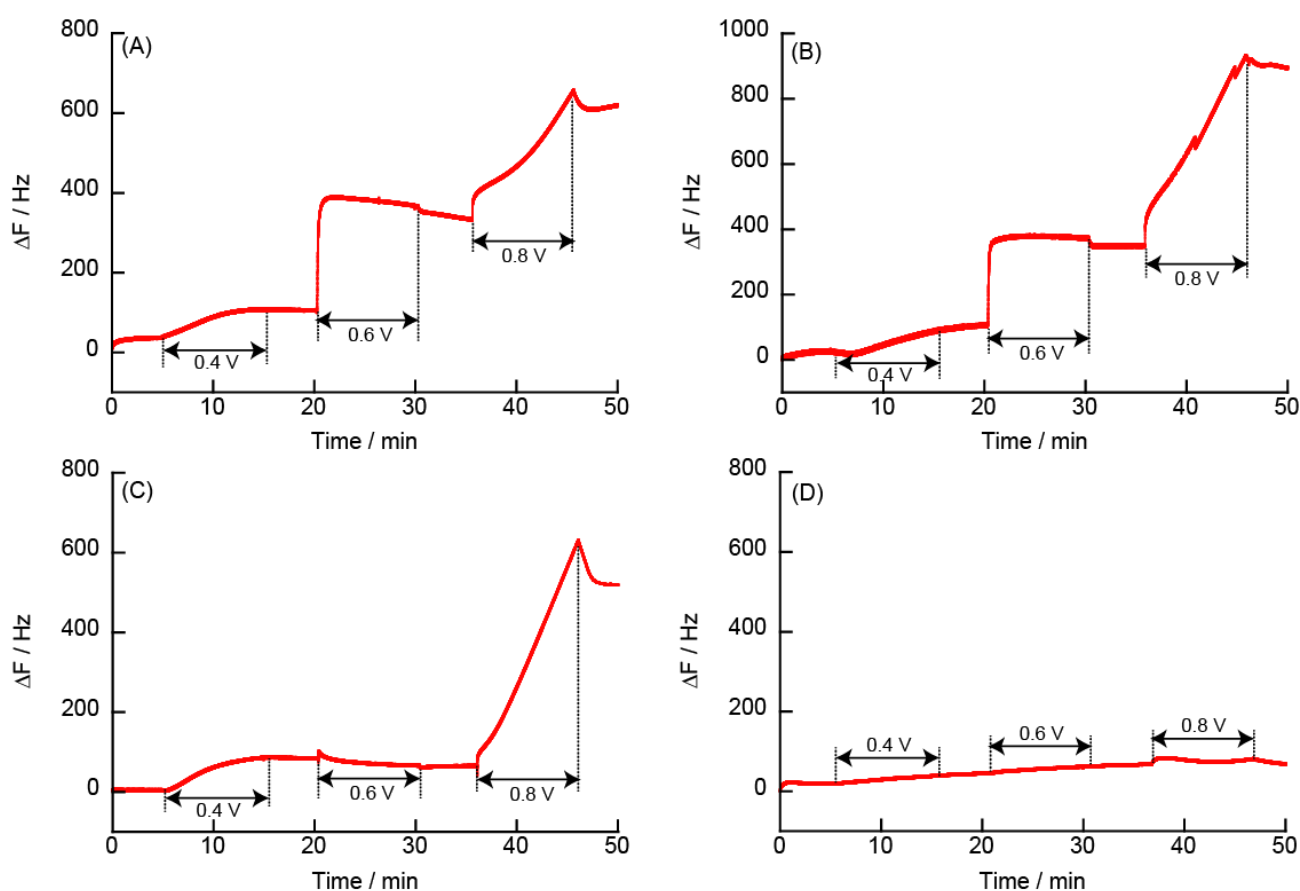


**Figure 11.** Changes in the resonance frequency for the (A) (PEI/TEMPO-PAA)<sub>5</sub>, (B) (PAH/TEMPO-PAA)<sub>5</sub>, (C) (PDDA/TEMPO-PAA)<sub>5</sub>, and (D) (PAMAM/TEMPO-PAA)<sub>5</sub> films with coating electrodes and constant potential. The electrode potential was applied at +0.4 V, +0.6 V, and +0.8 V for 10 min.

### 3.3. Release of FITC-Modified Polycations under Constant Potential

LbL films can contain drugs or can be made from polymer electrolytes such as insulin [36,37]. By skillfully using TEMPO derivatives, LbL films could be decomposed by electrical stimulation; therefore, we have investigated the possibility of application as a DDS. The polycations were labeled with FITC as a release model compound, and the release of FITC-polycations was evaluated from the fluorescence intensity of the solution in which the LbL films were electrically stimulated. Figure 12 shows the release of FITC-polycations upon application of +0, +0.4, +0.6, and +0.8 V to the (FITC-PEI/TEMPO-PAA)<sub>5</sub>, (FITC-PAH/TEMPO-PAA)<sub>5</sub>, and (FITC-PAMAM/TEMPO-PAA)<sub>5</sub> film-coated GCEs. FITC-PEI was released from the (FITC-PEI/TEMPO-PAA)<sub>5</sub> film by the application of +0.6 V

for 10 min. In the (FITC-PEI/TEMPO-PAA)<sub>5</sub> film, the amount of FITC-PEI released was increased with the potential from +0.4 V. Similar to the decomposition behavior of LbL films under low potential application, the release characteristics of FITC-PEI could also be controlled by manipulating the potential. However, the amount of FITC-PEI released was decreased when a potential of +0.8 V was applied. This is because FITC is oxidized to a non-fluorescent substance by the application of a potential [38]. If a DDS that is triggered by electric potential stimulation could be constructed, it would be necessary to do so at an electric potential at which the target drug does not undergo an electrochemical reaction. On the other hand, the (FITC-PAH/TEMPO-PAA)<sub>5</sub> and (FITC-PAMAM/TEMPO-PAA)<sub>5</sub> films did not show efficient decomposition by application of an electric potential. Although the amount of the (PAH/TEMPO-PAA)<sub>5</sub> film that was absorbed was larger than that of the (PEI/TEMPO-PAA)<sub>5</sub> film, the amount of FITC-PAH released was significantly smaller. Although the reason for this is still under investigation, it is speculated that the functional groups of PAHs are all primary amines and that they reacted with FITC upon application of the electric potential. Similar to the eQCM results, there was no release of FITC-PAMAM.

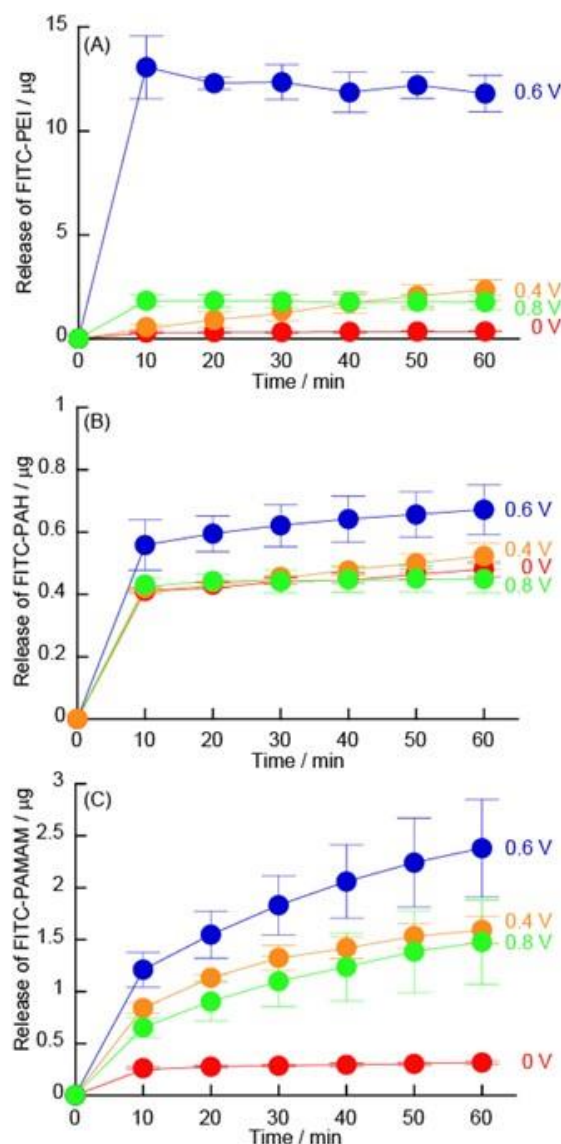


**Figure 12.** Release of (A) FITC-PEI from (FITC-PEI/TEMPO-PAA)<sub>5</sub>, (B) FITC-PAH from (FITC-PAH/TEMPO-PAA)<sub>5</sub> film, and (C) FITC-PAMAM from (FITC-PAMAM/TEMPO-PAA)<sub>5</sub> films coated on GCE at different constant potentials (red: 0 V, orange: +0.4 V, blue: +0.6 V, and green: +0.8 V).

#### 4. Conclusions

$E_p^a$  was observed around +0.6 V in CV measurements when a potential was applied to the (polycation/TEMPO-PAA) film-coated quartz resonator. This was due to the electrochemical oxidation of the TEMPO derivatives to generate oxoammonium ions [29]. At the same time, decomposition of the LbL films was observed at  $E_p^a$  around +0.6 V due to a sharp increase in  $\Delta F$ . It is considered that the oxoammonium ion has a positive charge, and the LbL films were decomposed due to electrostatic repulsion with the polycations (PEI, PAH, and PDDA). On the other hand, the CV of the (PAMAM/TEMPO-PAA)<sub>5</sub> film showed a small  $I_p^a$  during the 1st sweep scan, and the LbL film did not decompose. It is possible that the decomposition of the thin film is not promoted, probably because the amount of TEMPO-PAA absorbed is small. Furthermore, in the LbL films to which a constant potential was applied, decomposition was accelerated as the potential approached the  $E_p^a$  of TEMPO. However, when a constant potential of +0.8 V was applied, the release of FITC-modified polycations from the thin film was suppressed. It is possible that FITC and primary amines were electrochemically oxidized. If a DDS triggered by electric potential stimulation could be constructed, it would be necessary to do so at an electric potential at which the target drug does not undergo an electrochemical reaction. If the target drug does not cause an electrochemical reaction, it may be possible to construct DDS by electric potential stimulation.

**Supplementary Materials:** The following supporting information can be downloaded at: <https://www.mdpi.com/article/10.3390/polym14245349/s1>, Figure S1: UV-vis absorption spectra for the (PEI/TEMPO-PAA)<sub>5</sub> film (a) before and (b) after exposure to 1 mM sodium hypochlorite solution (pH 10) for 30 min.

**Author Contributions:** Conceptualization, K.Y., S.T. and K.S.; methodology and validation, K.Y.; Analysis of AFM, T.K.; resources, All co-authors; data curation, T.O. and T.D.; writing—original draft preparation, review and editing K.Y. and K.S.; supervision, Y.K.; project administration, K.Y. and K.S.; funding acquisition, K.Y., T.O., K.Y. and K.S. All authors have read and agreed to the published version of the manuscript.

**Funding:** Financial support from the Ou University Research Fund. This work was partially supported by a Grant-in-Aid for Scientific Research (No. 20K06984) from the Japan Society for the Promotion of Science (JSPS).

**Institutional Review Board Statement:** Not applicable.

**Data Availability Statement:** Not applicable.

**Acknowledgments:** The Ohu University Research Fund is also acknowledged for financial support. The authors thank the staff of Tsuruoka College for assisting with the atomic force microscopy observations.

**Conflicts of Interest:** The authors declare no conflict of interest.

#### References

1. Ariga, K. Progress in molecular nanoarchitectonics and materials nanoarchitectonics. *Molecules* **2021**, *26*, 1621. [[CrossRef](#)] [[PubMed](#)]
2. Ielo, I.; Giacobello, F.; Sfameni, S.; Rando, G.; Galletta, M.; Trovato, V.; Rosace, G.; Rosaria, M.P. Nanostructured surface finishing and coatings: Functional properties and applications. *Materials* **2021**, *14*, 2733. [[CrossRef](#)] [[PubMed](#)]
3. Gosecka, M.; Gosecki, M. Chemosensitive polymer systems for selective molecular recognition of organic molecules in biological systems. *Acta Biomater.* **2020**, *116*, 32–66. [[CrossRef](#)] [[PubMed](#)]
4. Lyu, X.; Gonzalez, R.; Horton, A.; Li, T. Immobilization of enzymes by polymeric materials. *Catalysts* **2021**, *11*, 1211.
5. Maksimkin, A.V.; Dayyoub, T.; Telyshev, D.V.; Gerasimenko, A.Y. Electroactive polymer-Based composites for artificial muscle-like actuators: A review. *Nanomaterials* **2022**, *12*, 2272. [[CrossRef](#)]
6. Arnon, H.; Granit, R.; Porat, R.; Poverenov, E. Development of polysaccharides-based edible coatings for citrus fruits: A layer-by-layer approach. *Food Chem.* **2015**, *166*, 465–472.

7. Ghiorghita, C.; Bucatariu, F.; Dragan, E.S. Influence of cross-linking in loading/release applications of polyelectrolyte multilayer assemblies. A review. *Mater. Sci. Eng. C* **2019**, *105*, 110050. [[CrossRef](#)]
8. Heuberger, L.; Korphidou, M.; Eggenberger, O.M.; Kyropoulou, M.; Palivan, C.G. Current perspectives on synthetic compartments for biomedical applications. *Int. J. Mol. Sci.* **2022**, *23*, 5718. [[CrossRef](#)]
9. He, Y.; Hong, C.; Li, J.; Howard, M.T.; Li, Y.; Turvey, M.E.; Uppu, D.S.S.M.; Martin, J.R.; Zhang, K.; Irvine, D.J.; et al. Synthetic Charge-invertible polymer for rapid and complete implantation of layer-by-layer microneedle drug films for enhanced transdermal vaccination. *ACS Nano* **2018**, *12*, 10272–10280.
10. Dubas, S.T.; Schlenoff, J.B. Swelling and smoothing of polyelectrolyte multilayers by salt. *Langmuir* **2001**, *17*, 7725–7727. [[CrossRef](#)]
11. Guzmán, E.; Ortega, F.; Rubio, R.G. Layer-by-layer materials for the fabrication of devices with electrochemical applications. *Energies* **2022**, *15*, 3399. [[CrossRef](#)]
12. Robert, S.C.; Kristine, S.E.; Urich, K.E. Synthesis and cytotoxicity of salicylate-based poly(anhydride esters). *Biomacromolecules* **2005**, *6*, 27–29.
13. Zhou, J.; Pishko, M.V.; Lutkenhaus, J.L. Thermoresponsive layer-by-layer assemblies for nanoparticle-based drug delivery. *Langmuir* **2014**, *30*, 5903–5910. [[CrossRef](#)]
14. Shi, D.; Ran, M.; Zhang, L.; Huang, H.; Li, X.; Chen, M.; Akashi, M. Fabrication of biobased polyelectrolyte capsules and their application for glucose-triggered insulin Delivery. *ACS Appl. Mater. Interfaces* **2016**, *8*, 13688–13697. [[CrossRef](#)]
15. Sato, K.; Imoto, Y.; Sugama, J.; Seki, S.; Inoue, H.; Odagiri, T.; Hoshi, T.; Anzai, J. Sugar-induced disintegration of layer-by-layer assemblies composed of concanavalin A and glycogen. *Langmuir* **2005**, *21*, 797–799. [[CrossRef](#)]
16. Yoshida, K.; Yamaguchi, A.; Midorikawa, H.; Kamijo, T.; Ono, T.; Dairaku, T.; Sato, T.; Fujimura, T.; Kashiwagi, Y.; Sato, K. Adsorption and release of rose bengal on layer-by-layer films of poly(vinyl alcohol) and poly(amidoamine) dendrimers bearing 4-carboxyphenylboronic acid. *Polymers* **2020**, *12*, 1854. [[CrossRef](#)]
17. Tokuda, Y.; Miyagishima, T.; Tomida, K.; Wang, B.; Takahashi, S.; Sato, K.; Anzai, J. Dual pH-sensitive layer-by-layer films containing amphoteric poly(diallylamine-co-maleic acid). *J. Colloid Interface Sci.* **2013**, *399*, 26–32.
18. Yoshida, K.; Kashimura, Y.; Kamijo, T.; Ono, T.; Dairaku, T.; Sato, T.; Kashiwagi, Y.; Sato, K. Decomposition of glucose-sensitive layer-by-layer films using hemin, DNA, and glucose oxidase. *Polymers* **2020**, *12*, 319. [[CrossRef](#)]
19. Yoshida, K.; Ono, T.; Dairaku, T.; Kashiwagi, Y.; Sato, K. Preparation of hydrogen peroxide sensitive nanofilms by a layer-by-layer technique. *Nanomaterials* **2018**, *8*, 941. [[CrossRef](#)]
20. Yoshida, K.; Awaji, K.; Shimizu, S.; Iwasaki, M.; Oide, Y.; Ito, M.; Dairaku, T.; Ono, T.; Kashiwagi, Y.; Sato, K. Preparation of microparticles capable of glucose-induced insulin release under physiological conditions. *Polymers* **2018**, *10*, 1164.
21. Takahashi, S.; Anzai, J. Recent Progress in Ferrocene-Modified Thin Films and Nanoparticles for Biosensors. *Materials* **2013**, *6*, 5742–5762. [[PubMed](#)]
22. Ma, W.; Zhang, Y.; Li, F.; Kou, D.; Lutkenhaus, J.L. Layer-by-layer assembly and electrochemical study of alizarin red s-based thin films. *Polymers* **2019**, *11*, 165. [[CrossRef](#)] [[PubMed](#)]
23. Cheng, Y.C.; Guo, S.L.; Chung, K.D.; Hu, W.W. Electrical Field-Assisted Gene Delivery from Polyelectrolyte Multilayers. *Polymers* **2020**, *12*, 133. [[CrossRef](#)] [[PubMed](#)]
24. Singh, P.; Parent, K.L.; Buttry, D.A. Electrochemical solid-state phase transformations of silver nanoparticles. *J. Am. Chem. Soc.* **2012**, *134*, 5610–5617. [[CrossRef](#)] [[PubMed](#)]
25. Ciriminna, R.; Ghahremani, M.; Karimi, B.; Pagliaro, M. Electrochemical alcohol oxidation mediated by TEMPO-like nitroxyl radicals. *ChemistryOpen* **2017**, *6*, 5–10.
26. Poizot, P.; Gaubicher, J.; Renault, S.; Dubois, L.; Liang, Y.; Yao, Y. Opportunities and challenges for organic electrodes in electrochemical energy storage. *Chem. Rev.* **2020**, *120*, 6490–6557.
27. Vereshchagin, A.A.; Kalnin, A.Y.; Volkov, A.I.; Lukyanov, D.A.; Levin, O.V. Key features of TEMPO-containing polymers for energy storage and catalytic systems. *Energies* **2022**, *15*, 2699.
28. Rozantzev, E.G.; Neiman, M.B. Organic radical reactions involving no free valence. *Tetrahedron* **1964**, *20*, 131–137. [[CrossRef](#)]
29. Semmelhack, M.F.; Chou, C.S.; Cortes, D.A. Nitroxyl-mediated electrooxidation of alcohols to aldehydes and ketones. *J. Am. Chem. Soc.* **1983**, *105*, 4492–4494. [[CrossRef](#)]
30. Takahashi, S.; Aikawa, Y.; Kudo, T.; Ono, T.; Kashiwagi, Y.; Anzai, J. Electrochemical decomposition of layer-by-layer thin films composed of TEMPO-modified poly(acrylic acid) and poly(ethyleneimine). *Colloid Polym. Sci.* **2014**, *292*, 771–776.
31. Watanabe, K.; Sugiyama, K.; Komatsu, S.; Yoshida, K.; Ono, T.; Fujimura, T.; Kashiwagi, Y.; Sato, K. Voltammetric pH measurements using azure A-containing layer-by-layer film immobilized electrodes. *Polymers* **2020**, *12*, 2328.
32. Craig, M.; Holmberg, K.; Ru, E.L.; Etchegoin, P. Polypeptide multilayer self-assembly studied by ellipsometry. *J. Drug Deliv.* **2014**, *2014*, 424697. [[CrossRef](#)]
33. Ciejka, J.; Grzybala, M.; Gut, A.; Szuwarzynski, M.; Pyrc, K.; Nowakowska, M.; Szczubialka, K. Tuning the surface properties of poly(allylamine hydrochloride)-based multilayer films. *Materials* **2021**, *14*, 2361.
34. Chauhan, A.S. Dendrimers for drug delivery. *Molecules* **2018**, *23*, 938.

35. Kheraldine, H.; Rachid, O.; Habib, A.M.; Al Moustafa, A.E.; Benter, I.F.; Akhtar, S. Emerging innate biological properties of nano-drug delivery systems: A focus on PAMAM dendrimers and their clinical potential. *Adv. Drug Deliv. Rev.* **2021**, *178*, 113908. [[CrossRef](#)]
36. Yoshida, K.; Hasebe, Y.; Takahashi, S.; Sato, K.; Anzai, J. Layer-by-layer deposited nano- and micro-assemblies for insulin delivery: A review. *Mater. Sci. Eng. C* **2014**, *34*, 384–392.
37. Díez-Pascual, A.M.; Rahdar, A. LbL Nano-assemblies: A versatile tool for biomedical and healthcare applications. *Nanomaterials* **2022**, *12*, 949. [[CrossRef](#)]
38. Queiroz, N.L.; Nascimento, J.A.M.; Nascimento, M.L.; Nascimento, V.B.; Oliveira, S.C.B. Oxidation Mechanism of Fluorescein at Glassy Carbon Electrode. *Electroanalysis* **2017**, *29*, 489–496. [[CrossRef](#)]